Title
MEASUREMENT OF ELECTRON BEAM POLARIZATION AT THE SLC

Author
Steiner, H.

Publication Date
1987-03-01

Lawrence Berkeley Laboratory
UNIVERSITY OF CALIFORNIA

Physics Division

Presented at the International Conference on
Advances in Experimental Methods for Colliding
Beam Physics, Stanford, CA, March 9–13, 1987

MEASUREMENT OF ELECTRON BEAM POLARIZATION AT THE SLC

H. Steiner

March 1987

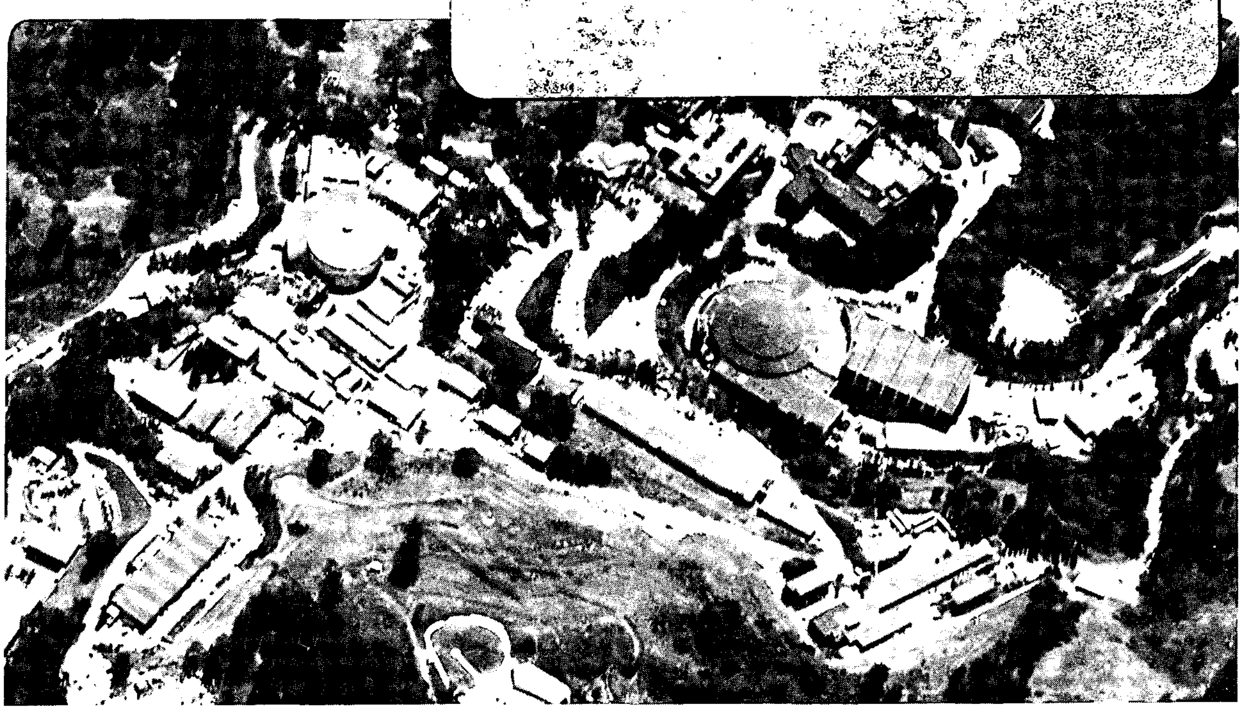

Prepared for the U.S. Department of Energy under Contract DE-AC03-76SF00098

LBL-23452

Presented at the International Conference on Advances in Experimental Methods for Colliding Beam Physics, March 9–13, 1987, SLAC, Stanford, CA

MEASUREMENT OF ELECTRON BEAM POLARIZATION AT THE SLC

Herbert Steiner

Lawrence Berkeley Laboratory
and Department of Physics
University of California
Berkeley, CA 94720

This work was supported by the Director, Office of Energy Research, Office of High Energy and Nuclear Physics, Division of High Energy Physics of the U.S. Department of Energy under contract DE-AC03-76SF00098.

MEASUREMENT OF ELECTRON BEAM POLARIZATION AT THE SLC

Herbert Steiner
Lawrence Berkeley Laboratory and Department of Physics
University of California, Berkeley, CA 94720

I. Introduction

One of the unique features of the SLC is its capability to accelerate longitudinally polarized electrons. These can be used to test the Standard Model of Electroweak Interactions with unprecedented accuracy. The SLC polarization group[1] consisting of physicists and engineers from SLAC, LBL, Indiana University, and the University of Wisconsin has been formed to implement the polarization program at the SLC. The SLAC management has approved a schedule which calls for installation of the polarization option in summer 1988.

Technically the polarization project consists of three main parts: (1) a polarized source, (2) spin-rotating superconducting solenoid magnets to be used to manipulate the direction of the electron spin, and (3) the polarimeters needed to monitor and measure the electron beam polarization. It is this last topic that will concern us here.

Two types of polarimeters will be used—Compton and Moeller. The first of these is based on the fact that the elastic scattering of photons from high energy electrons is strongly spin dependent, whereas the second utilizes the spin dependence of elastic electron-electron scattering. The advantage of the Compton method is that it has very high analyzing power and thus should permit high precision, whereas the virtue of the Moeller method is its relative simplicity and high data rate. The use of these two independent methods which have largely uncorrelated systematic errors is expected to yield reliable values for the beam polarization.

The polarimeters will have two main functions. On the one hand they will be used to make quick relative measurements for purposes of monitoring and diagnostics. Such measurements are intended to be fully compatible with normal SLC operation in the colliding mode. Accuracies of less than 1% should be attainable in less than a minute. The other function is to use the polarimeters to make occasional high precision absolute measurements for calibration. At least some of these measurements will involve short dedicated runs with only the electron beam. Initially we hope to achieve 5% accuracy in the absolute polarization determination, with a goal of reaching 1% after we have gained enough experience.

A schematic layout of the SLC including the main polarization components is shown in figure 1. There are Moeller polarimeters at the end of the linac and in the extraction-line spectrometer, and a Compton polarimeter about 40 meters south of the electron-positron interaction point (IP).

In the following sections the plans of the SLC polarization group to measure and monitor electron beam polarization will be discussed in greater detail. Section II is devoted to a brief discussion of the physics and the demands it imposes on beam polarization measurements. The Compton polarimeter is described in section III. The essential characteristics of the two Moeller polarimeters are presented in section IV.

II. Physics with Polarized Electrons

The Standard Model of electroweak interactions is phrased in terms of left-handed and right-handed particles whose couplings are not identical but are completely determined by knowledge of three fundamental parameters: The fine structure constant, α, the Fermi Coupling constant, G_F, and the mass of the Z, m_Z.

One of the first tasks at the SLC will be the accurate measurement of m_Z. The extraction-line spectrometers[2] will be used to measure the energy of the electron and positron beams to better than 1 part in a thousand, and thereby to determine the mass of the Z to about 45 MeV. When longitudinally polarized electrons become available the energy- dependent spin precession in the arcs will cause the spins of 50 GeV electron to make about 28 complete revolutions between the end of the linac and the electron-positron interaction point. This spin precession can be used to make an independent calibration of the energy of the electron beam with a precision which is comparable to that obtainable with the extraction-line spectrometer.

Once the three basic parameters of the theory are known it uniquely predicts all other observables. The most stringent test of the Standard Model can be made by using longitudinally polarized electrons to measure the left-right asymmetry.

$$A_{LR} = \frac{\sigma_L - \sigma_R}{\sigma_L + \sigma_R}$$

Here left (right) refers to negative (positive) helicity electrons, and σ can be any total or partial cross section for any process. Figure 2 shows how well A_{LR} can be determined with a given number of Z's, and how such a measurement of A_{LR} translates into a determination of the value of $sin^2\theta_W$ and its error, or equivalently the value and error on m_Z. These results are indicated on the right-hand scales, assuming 45% beam polarization and a measurement of beam polarization known to 5% (solid line), 3% (dot-dashed line), and 1% (dashed line). Only when the beam polarization measurements achieve an accuracy of <1% do we realize the full potential of this powerful method. Once a statistical sample of 10^6 Z's decays has been obtained the accuracy with which the beam polarization can be determined will be the limiting factor in testing the Standard Model.

The asymmetry measurements become especially interesting if the statistical and systematic errors can be pushed below the 1% level, because the effects of new physics, such as the existence of supersymmetric particles, heavy Higgses, new heavy quarks, new heavy gauge bosons, etc., have been calculated[3] to produce ~1% deviations from the predictions of the "pure" standard model. Thus it is our goal to develop polarimeters capable of measuring absolute electron beam polarization to better than

1%. We are also striving to develop a polarized source which can deliver 90-100% polarized electrons rather than the 45% expected with the present source.

III. The Compton Polarimeter

III.A. Method

The basic idea of the proposed Compton Polarimeter is to backscsatter circularly polarized laser photons from the electrons of the SLC about 33 meters south of the intersection point of the electron and positron beams. The method utilizes the fact that the Compton cross sections for parallel and anti-parallel electron-photon helicities are very different. To minimize the background we have chosen to detect and measure the momentum of the scattered electron rather than the photon. The location of the polarimeter was chosen to be (1) along a straight line from the electron-positron intersection point so as to avoid energy-dependent spin precession, (2) near an intermediate focus of the electron beam to maximize luminosity, and (3) immediately before beam-bending magnets SB1 and B1 in order to utilize them to momentum analyze the Compton scattered electrons. A schematic diagram is shown in figure 3.

The analyzing power for circularly polarized 2.34 eV ($\lambda = 532$ nm) photons on 50 GeV longitudinally polarized electrons as a function of the lab energy of the recoil electron is shown in figure 4a. Figure 4b shows the same function when the photon's energy is 4.0 eV ($\lambda = 308$ nm). These are the wavelengths produced by a frequency-doubled Nd:YAG laser or a XeCl excimer laser, respectively. Several points are worthy of note: (1) the recoil energy of the electron can be less than half of the beam energy, (2) the maximum asymmetry is large, (3) the asymmetry decreases and passes through 0 as the energy of the scattered electron increases (or equivalently, as the center-of mass scattering angle decreases), (4) there is a well defined minimum recoil energy. As will be discussed later the latter two features are useful for calibration purposes.

The relevant cross sections are large enough that commercially available lasers are sufficiently intense to produce a reasonable interaction rate. Rapid and essentially bias-free reversals of photon and/or electron polarization will minimize most systematic effects. The scattered electrons are contained in a cone of half-angle less than 10 microradians with respect to the beam axis. Our detection scheme is based on using magnets SB1 and B1 to momentum analyze these scattered electrons (thereby also separating them from the electron beam), and thereafter to measure their position in a segmented threshold Cherenkov detector. This detector, to be described below, is designed to be largely insensitive to the flood of low energy photons coming from synchrotron radiation and beamstrahlung in this region of the accelerator.

The Compton polarimeter will be used both as an on-line monitor of the electron beam polarization, and for precise measurement of the magnitude of this polarization. In the monitoring mode we can collect enough data for 1% statistical accuracy within a few seconds at the design beam current of 5×10^{10} electrons per pulse. For the precision measurement of absolute polarization we intend to run at least some of the time with the beams in the non-colliding mode. This mode of operation removes important sources of background such as radiative Bhabha scattering and beamstrahlung. It also results in a smaller electron beam and hence better Compton luminosity. But even in the presence of colliding electron and positron beams the polarimeter is expected to achieve high accuracy.

III.B. The Laser System

We intend to use a XeCl excimer laser having a peak power of 20 MW at ($\lambda =$ 308 nm) with a pulse width of 8 ns and a repetition rate of up to 180 Hz. Some initial tuning and debugging will probably be done with a frequency-doubled Nd:YAG laser which is already available to us. The laser(s), together with the polarizing elements and beam synchronization electronics, will be housed in a small alcove which is accessible during normal operation of the SLC (see figure 5). An optical beam transport system consisting of a series of pairs of 90 degree reflectors which maintains the full circular polarization of the laser beam will be used to transport to laser light from its source to the intersection point with the electron beam. At the CIP (Compton Intersection Point) the angle between the laser beam direction and the electron beam direction is $(\pi - 0.020)$ radians. After passing the CIP the laser beam will be brought out of the SLC vacuum and its intensity, position, polarization, and time structure will be monitored.

III.C. The Cherenkov Detector

Perhaps the greatest unknown at this point in time is the radiation environment near the polarimeter, and the backgrounds that will be generated in our detector. Because we expect the detector to be permeated by a flood of low energy photons from scattered synchrotron radiation and beamstrahlung we have chosen to use a segmented threshold gas Cherenkov counter to detect the Compton scattered electrons. This detector will be insensitive to electrons of 10 MeV or less when operated with β-butylene gas at atmospheric pressure. The threshold can of course be varied by changing the pressure or the type of gas. It has been shown by Heintze, et al.[4] and verified by us that β-butylene has one of the lowest scintillating efficiencies of any gas in the wavelength region to which our phototubes are sensitive. The fact that Cherenkov light is strongly collimated whereas scintillation light is isotropic provides us with another powerful means of rejecting background.

In figure 6 we schematically show the paths of the momentum-analyzed Compton scattered electrons as they pass through our Cherenkov detector. The electrons having the greatest asymmetry are those with the lowest energy which are furthest from the 50 GeV electron beam. Our detector is being designed to accept electrons ranging in momentum from 33 GeV/c (about 3 cm from the beam) to 12.5 GeV/c (about 19 cm from the beam) in 40 equal width segments, each of which is viewed by a small photomultiplier tube. In the high-asymmetry region the energy of the recoil electrons can be determined to 0.1 GeV. The kinematic limit corresponding to maximum momentum transfer as well as the energy where the asymmetry goes to zero will be used to calibrate the system (see figure 4).

The Cherenkov light produced by the Compton scattered electrons will be emitted into a cone of half angle 0.05 radians, and will produce about one detectable photon per centimeter. The light will be channeled by thin reflecting strips spaced 4mm apart for a length of 20cm, and then be reflected by individual small mirrors oriented at about 45 degrees to photmultiplier tubes which we plan to locate in an adequately shielded region below the beam line. (See figure 7). With a beam current of 5×10^{10} electrons per pulse we expect to detect about 100 Compton scattered electrons per pulse. This number could be increased by using a laser of higher intensity and/or by putting a few radiation lengths of material immediately in front of the detector so that the incident electrons produce showers. EGS calculations indicate that about an order of magnitude increase in gain can be obtained with a few centimeters of lead without seriously degrading the spatial resolution of the detector.

III.D. The Multiwire Proportional Chamber

Compton scattered electrons having energies less than 30% of the beam energy are bent sufficiently by bending magnets SB1 and B1 to pass to the left of quadrupole Q7. These electrons are of particular interest because they exhibit the largest spin-dependent asymmetry (see figure 4b). After passing through our Cherenkov detector they will also be detected by a small multiwire proportional chamber located in the low background region behind Q7. Both the Cherenkov detector and the wire chamber can be used simultaneously when no converting material is placed in front of the Cherenkov detector. The readout of the wire chamber will integrate the total charge collected as a function of position in the detector.

III.E. Use of the Cherenkov Detector as a Relative Luminosity Monitor

In the region of the Cherenkov detector near the beam, where the detected electrons have more than half of the beam energy, we expect the Compton signal to be overwhelmed by electrons coming from radiative Bhabha scattering at the IP. These electrons, whose energy spectrum falls steeply as their energy falls below the beam energy, will be a serious luminosity-dependent source of background. For once, however, we hope to use a background to our advantage. The copious radiative Bhabha events should allow us to use this region of the detector as a high-rate relative luminosity monitor. It is a relative monitor because the beam transport system will be badly mistuned for these lower energy electrons, and only a small energy-dependent fraction of them will actually reach our detector. From the point of view of Compton polarimetry this kinematic region is of interest mainly for purposes of calibration, and we intend to make such calibrations when the beams are not colliding. The kinematic region of greatest interest in determining the beam polarization is where the asymmetry is largest. This occurs when electrons have less than half of the beam energy. In this region the radiative Bhabha background is expected to be tolerably small even at the design luminosity of $6 \times 10^{30} cm^{-2} sec^{-1}$.

III.F. Status

The present status is that a laser is being readied for tests in the laboratory, the optical beam transport system is being designed, and a single-channel prototype Cherenkov counter has been built and tested in a 90 MeV electron test beam. Within the next few months we plan to install this prototype detector as well as another one having several cells in the region of the SLC foreseen for the full-scale detector. These prototype detectors may well be suitable for use as relative luminosity monitors during the early stages of SLC operation. Only after we learn more about the backgrounds and how the prototype detectors perform *in situ* will we proceed with the design and construction of the actual detector. We would like to install this detector in fall 1987 or early 1988.

IV. The Moeller Polarimeters

IV.A. Method

Moeller scattering has been used in previous experiments at SLAC to measure electron beam polarizations. It is a well understood QED process and a well understood experimental technique. The monitoring of polarized beams through the proper use of the spin-dependent terms in the Moeller process provides a rapid and precise measure of polarization. Figure 8 illustrates schematically the layout of a Moeller polarimeter for high energy polarized electron beams. An electron beam incident on a thin target, scatters from the quasi-free atomic electrons in the material. Relativistic kinematics for the high energies dictates forward scattering at small angles for both the incident and target electrons. For SLC beam energies, the symmetric angle, corresponding to each electron having $E_{beam}/2$ at 90° in the center-of-mass, is about 4.6 milliradians. The forward going electrons are easily separated from the unscattered beam by a magnet, illustrated in figure 8, and deflected into a detector such as a PWC hodoscope. The two-body kinematics give a relation between momentum p and and angle θ for the scattered electron. The PWC hodoscope sees a Moeller signal falling in only a few bins of the hodoscope. Figure 9a shows data obtained in a SLAC experiment in 1978. The Moeller peak is clear, sitting on a 25% background which comes from the radiative tail of e-Fe nucleus scattering. The polarization of the beam is measured by polarizing the target, and observing the asymmetry for spins aligned parallel versus anti-parallel. An asymmetry is defined by

$$A = (N_p - N_a)/(N_p + N_a)$$

where $N_p(N_a)$ is the number of detected electrons when spins are aligned parallel (anti-parallel). This asymmetry can be formed when one flips the beam polarization or the target polarization. Figure 9b shows the bin-to-bin asymmetries observed in a typical one-minute-long run in the SLAC 1978 experiment. The analyzing power of the polarized target was about 5.6%, showing that the beam polarization for these data was around 0.40. The accuracy of this type of measurement was about ± 0.02.

Moeller polarimeters for the SLC will be installed at the end of the linac and, as part of the extraction-line spectrometer system, near the electron beam dump. The latter location is not ideal, being separated from the IP by 150 meters and several magnetic bends, but it has the advantage of utilizing an existing system of magnets, and it allows the polarimeter to reside continually in the beam without interfering with machine or experimental operations. Spin precession between the IP and this Moeller polarimeter is relatively large, and the spin orientation at the monitor will not be the same as at the IP. However spin motion is determined by the beam energy and the magnetic fields, and the measurement can be related to the value at the IP by a simple matrix relationship. For this reason, and the fact that spin at the IP will not be purely longitudinal, the Moeller spectrometer will be designed to measure all three components of the spin. This can be accomplished with the same detector and spectrometer by suitable orientation of the target foil.

With the SLC running at the design current of 5×10^{10} electrons per pulse and a pulse rate of 120 Hz it should be possible to measure the polarization of the electron beam with a statistical accuracy of less than 1% in a few minutes of running. Systematic errors of comparable magnitude are expected. These are due mainly to uncertainties associated with determination of the target polarization and with clean isolation of the Moeller-scattered signal; i.e., background subtraction.

IV.B. The Target

The Moeller target is a magnetized foil of a high-permeability magnetic material. Previous targets used successfully the material SUPERMENDUR, which is an iron-cobalt-nickel alloy. It saturates magnetically around 100 gauss external field. Thin sheets of this material magnetize with spin components preferentially in the plane of the sheet. The foil sits at an angle with respect to the beam. For longitudinal spins, the normal to the sheet forms an angle of 70° to the beam (i.e., nearly edgewise to the beam), while for transverse measurements, the normal to the plane coincides with the beam axis. External magnetic fields from a simple pair of coils bias the foils in the desired direction. Fields of a few hundred gauss are adequate. Figure 10 shows the orientation of the targets and placement of coils for longitudinal and transverse measurements.

IV.C. The Detector

The parameters of importance are sensitivity to electrons, fine angular resolution, and ability to operate at high incident rates. The detector used in the Moeller spectrometer in the earlier SLAC work consisted of a PWC hodoscope in a brass body, behind 1 X_0 of lead. Using the high voltage, the gain was adjustable, so proper operating points could be found for all beam conditions. Signals from each PWC wire were integrated and digitized. In the computer, asymmetries were formed and sorted for each PWC channel. Figure 11 shows a sketch of the detector.

IV.D. Status

The extraction-line spectrometer is scheduled for installation in the fall of 1987. The detailed design of the Moeller polarimeter presently underway. Construction of the target assembly and the detector will take place during the second half of 1987. It may be possible to commence installation of the polarimeter in late 1987, but in any case we intend it to be fully installed before the end of summer 1988.

Figure Captions

Figure 1: Schematic layout of SLC showing the location of the main polarization components.

Figure 2: The uncertainty in the left-right asymmetry, ΔA_{LR}, as a function of the number, N, of observed Z decays. The three curves correspond to $\Delta P/P = 5\%, 3\%, 1\%$. The uncertainty includes the effect of $\Delta P/P$ and of statistics, but not the theoretical uncertainty.

Figure 3: Schematic layout of Compton polarimeter.

Figure 4: Asymmetry in Compton scattering vs. recoil electron energy for (a)532 nm (b) 308 nm photons on 50 GeV electrons.

Figure 5: Location of Compton polarimeter and laser vault relative to the SLC experimental hall.

Figure 6: Trajectories of Compton recoil electrons of various energies in the vicinity of the Cherenkov detector. Floor position is transverse to the beam.

Figure 7: Schematic diagram of Cherenkov detector. Side view.

Figure 8: Schematic view of the Moeller polarimeter in the extraction line spectrometer. Three magnets are shown, two with horizontal bends and one which bends vertically. The horizontal bends are of no significance to the Moeller polarimeter. The vertical bend disperses the Moeller scattered electrons in a vertical direction. A detector placed approximately 12 meters downstream detects the Moeller signal. Slits in front of the first magnet are used to define the azimuthal acceptance.

Figure 9: Moeller scattering data from an early SLAC experiment:

(a) cross section vs scattering angle (scales relative) showing the Moeller peak on a background from electron-Fe scattering;

(b) The asymmetry on an absolute scale corresponding to approximately 40% polarization.

Figure 10: Schematic view showing the orientation of the target, beam, and magnetic field for measuring the longitudinal and transverse components of beam polarization.

Figure 11: Sketch of a possible Moeller detector.

References

(1) D. Blockus et al., "Proposal for Polarization at the SLC" (K. C. Moffeit, H. Steiner, co-spokespersons) 1986.

(2) M. Levy, private communication.

(3) B. W. Lynn, M. E. Peskin, and R. G. Stuart, SLAC-PUB-3725; M. Cvetic and

B. W. Lynn, Phys. Rev. D35:51 (1987).

(4) J. Heintze, K. Kalbreier, H. Rieseberg, H. W. Siebert and K.-P. Streit, NIM138: 641 (1976).

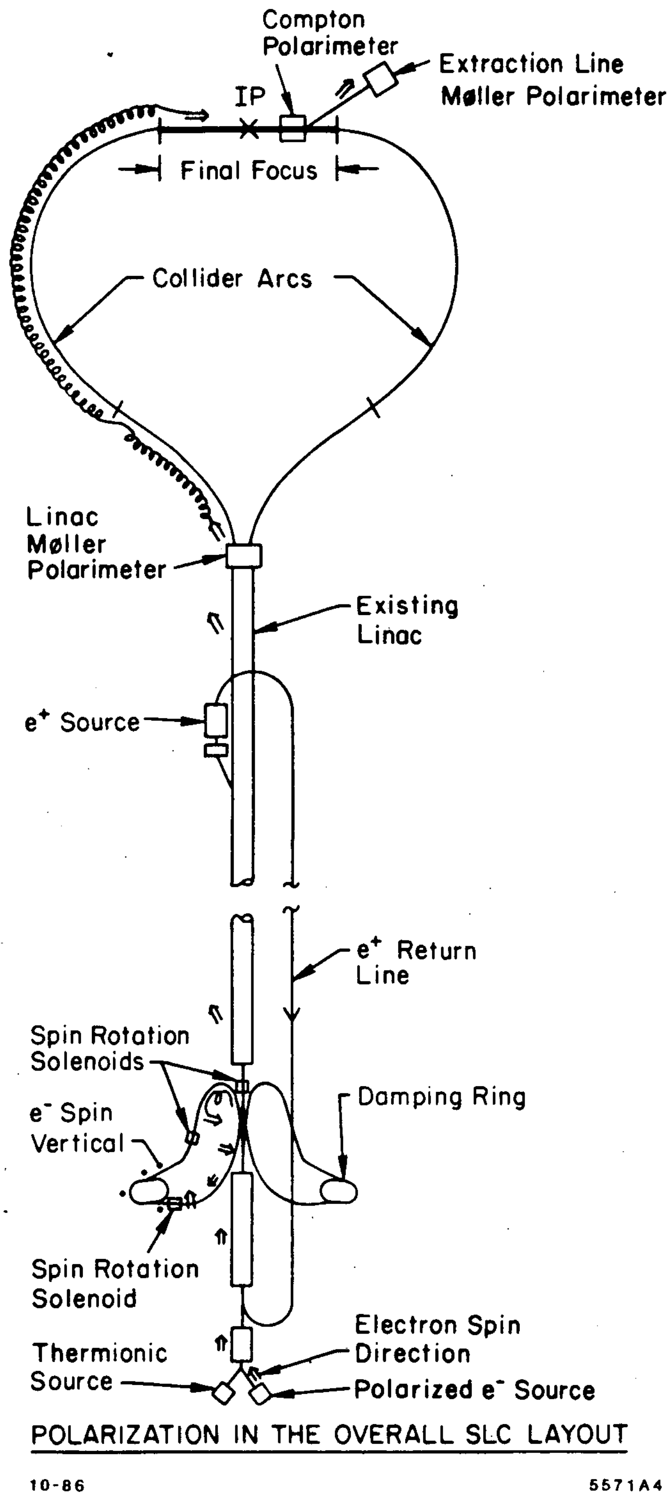
Compton
Polarimeter
Extraction Line
Møller Polarimeter
IP
Final Focus
Collider Arcs
Linac
Møller
Polarimeter
Existing
Linac
e+ Source
e+ Return
Line
Spin Rotation
Solenoids
e- Spin
Vertical
Damping Ring
Spin Rotation
Solenoid
Electron Spin
Direction
Thermionic
Source
Polarized e- Source
POLARIZATION IN THE OVERALL SLC LAYOUT
10-86
5571A4

Fig. 1

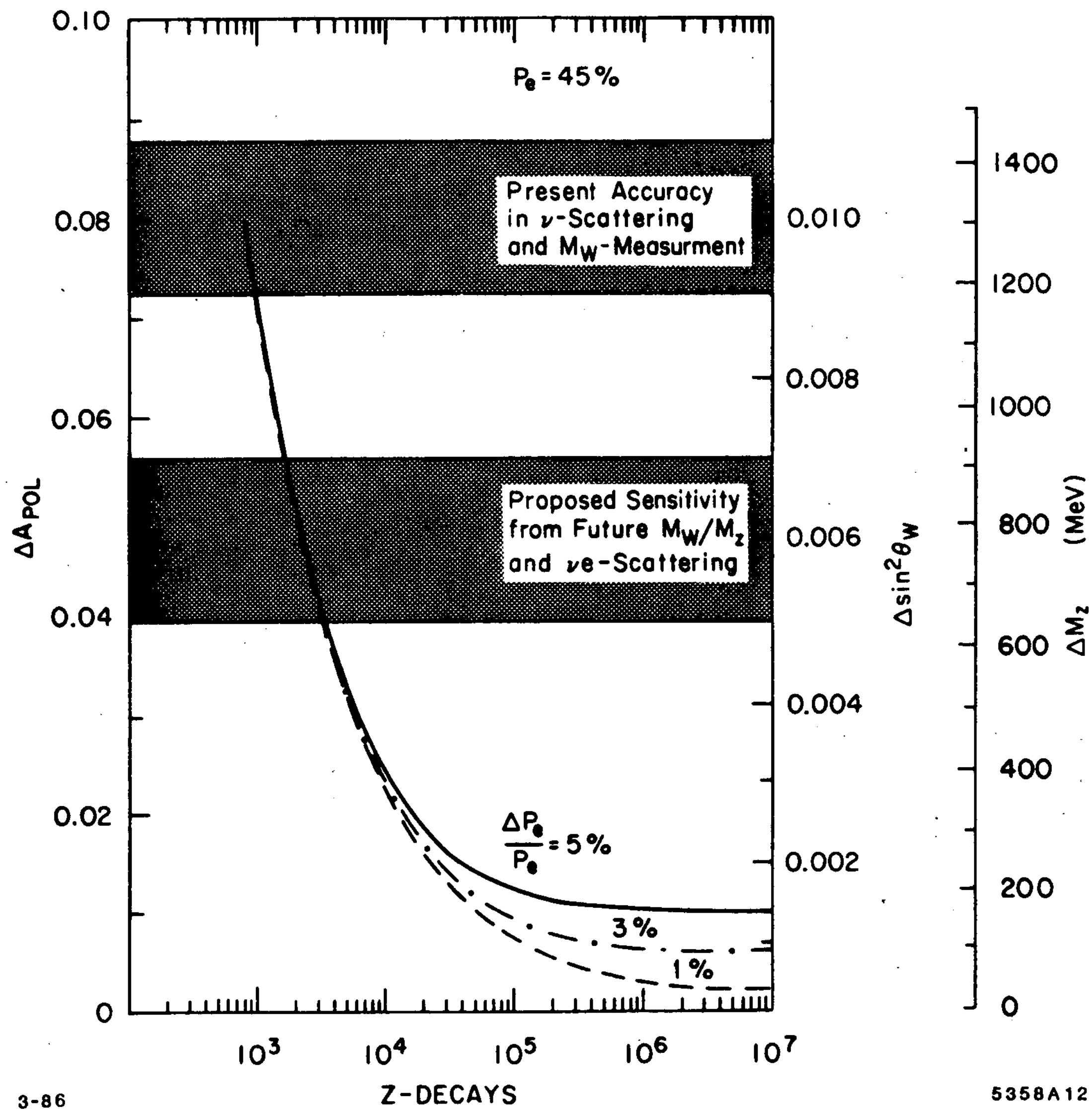

0.10
0.08
0.06
0.04
0.02
0
ΔA_{POL}
$P_e = 45\%$
Present Accuracy
in ν-Scattering
and M_W-Measurment
Proposed Sensitivity
from Future M_W/M_z
and νe-Scattering
$\frac{\Delta P_e}{P_e} = 5\%$
3%
1%
0.010
0.008
0.006
0.004
0.002
$\Delta \sin^2\theta_W$
1400
1200
1000
800
600
400
200
0
ΔM_z (MeV)
10^3
10^4
10^5
10^6
10^7
Z-DECAYS
3-86
5358A12

Fig. 2

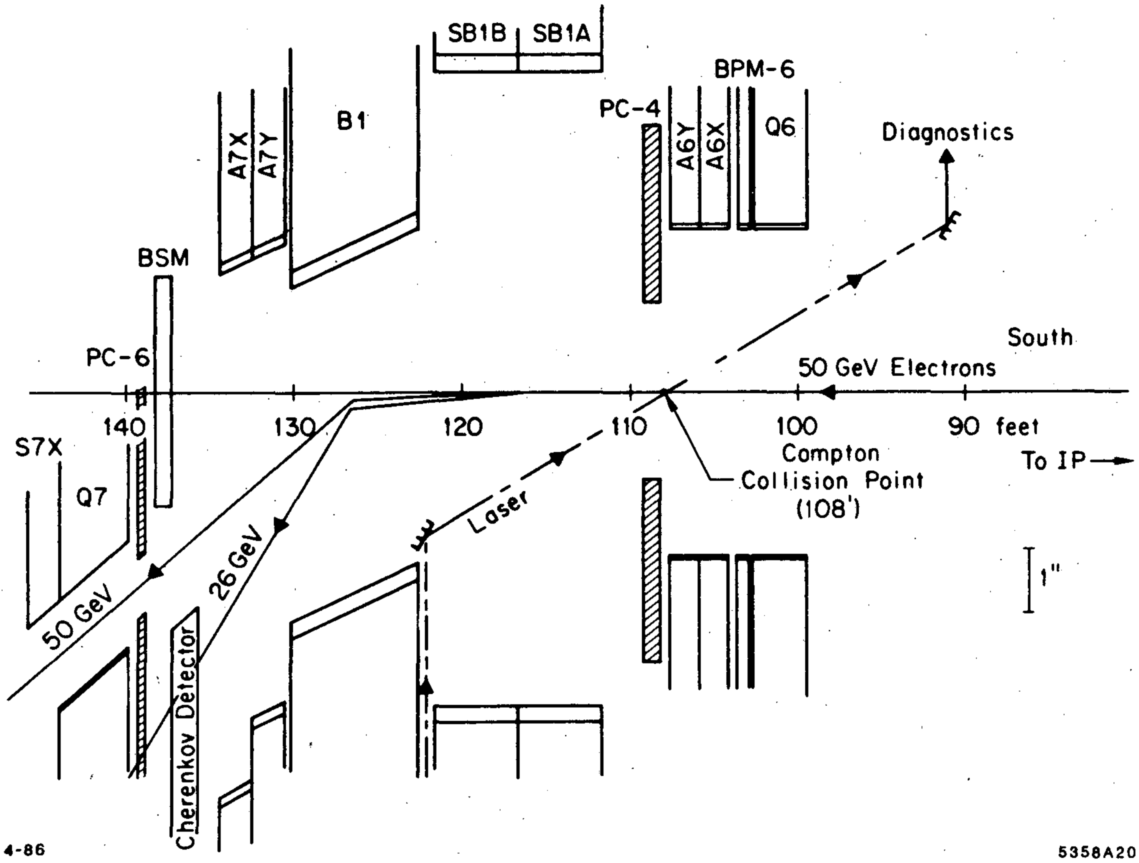
SB1B
SB1A
BPM-6
B1
PC-4
Q6
Diagnostics
A7X
A7Y
A6Y
A6X
BSM
South
PC-6
50 GeV Electrons
140
130
120
110
100
90 feet
S7X
Compton
To IP
Q7
Collision Point
(108')
Laser
26 GeV
1"
50 GeV
Cherenkov Detector
4-86
5358A20

Fig. 3

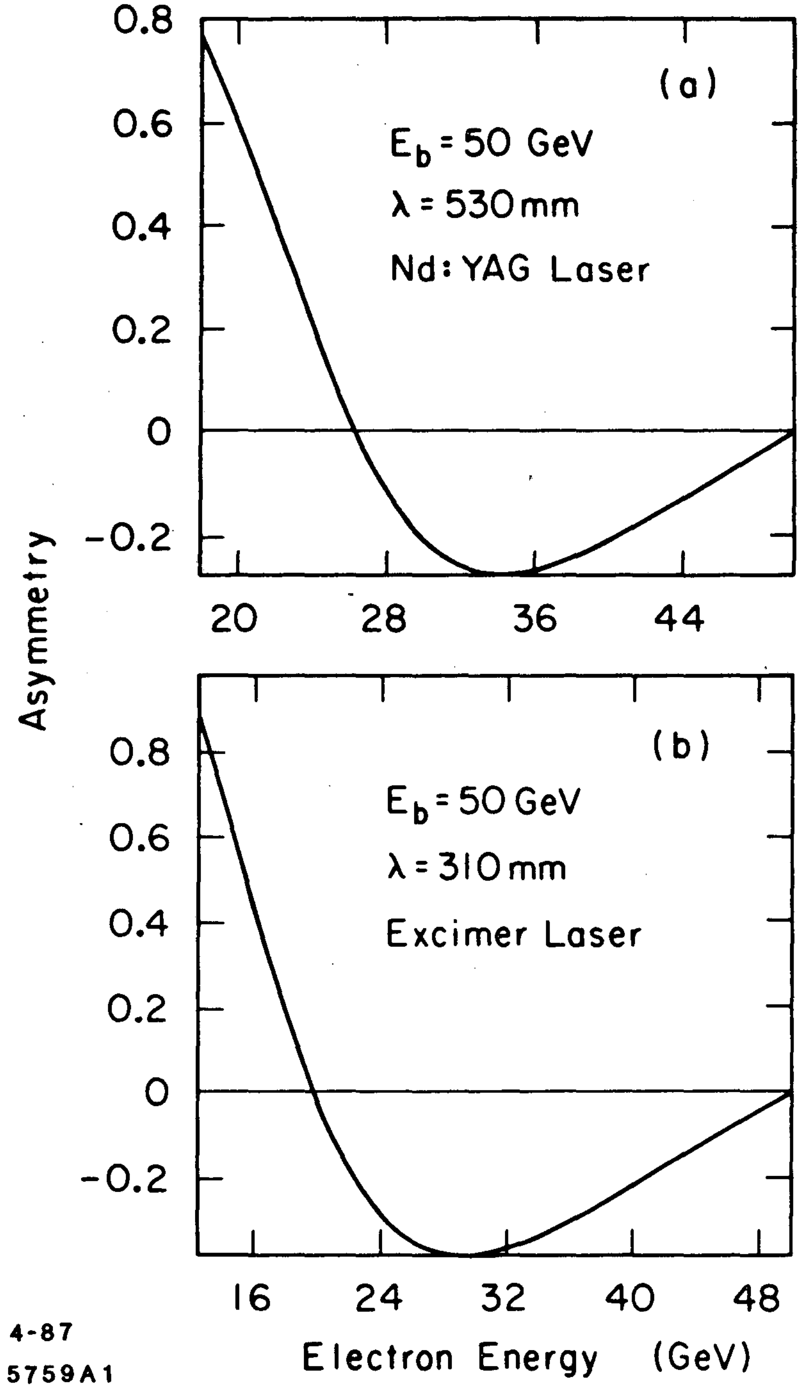

(a)
E_b = 50 GeV
λ = 530 mm
Nd: YAG Laser
0.8
0.6
0.4
0.2
0
-0.2
20
28
36
44
Asymmetry
(b)
E_b = 50 GeV
λ = 310 mm
Excimer Laser
0.8
0.6
0.4
0.2
0
-0.2
16
24
32
40
48
Electron Energy (GeV)
4-87
5759A1

Fig. 4

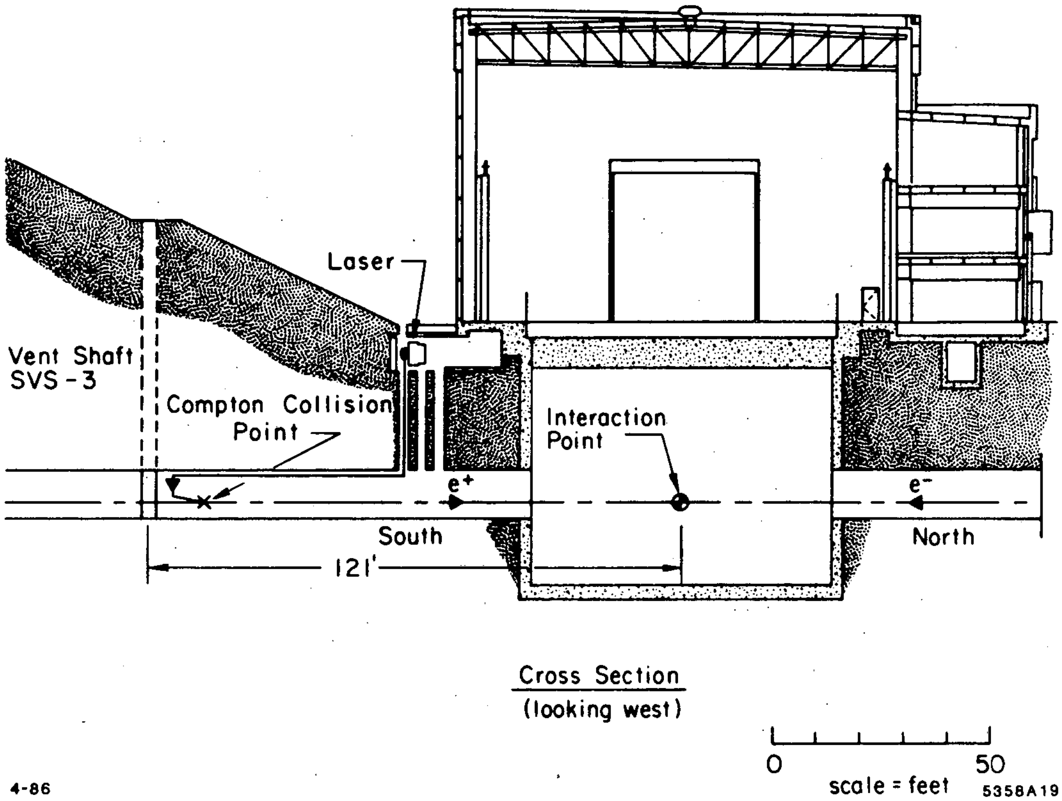
Laser
Vent Shaft
SVS - 3
Compton Collision
Point
Interaction
Point
e+
e-
South
North
121'
Cross Section
(looking west)
0
50
scale = feet
4-86
5358A19

Fig. 5

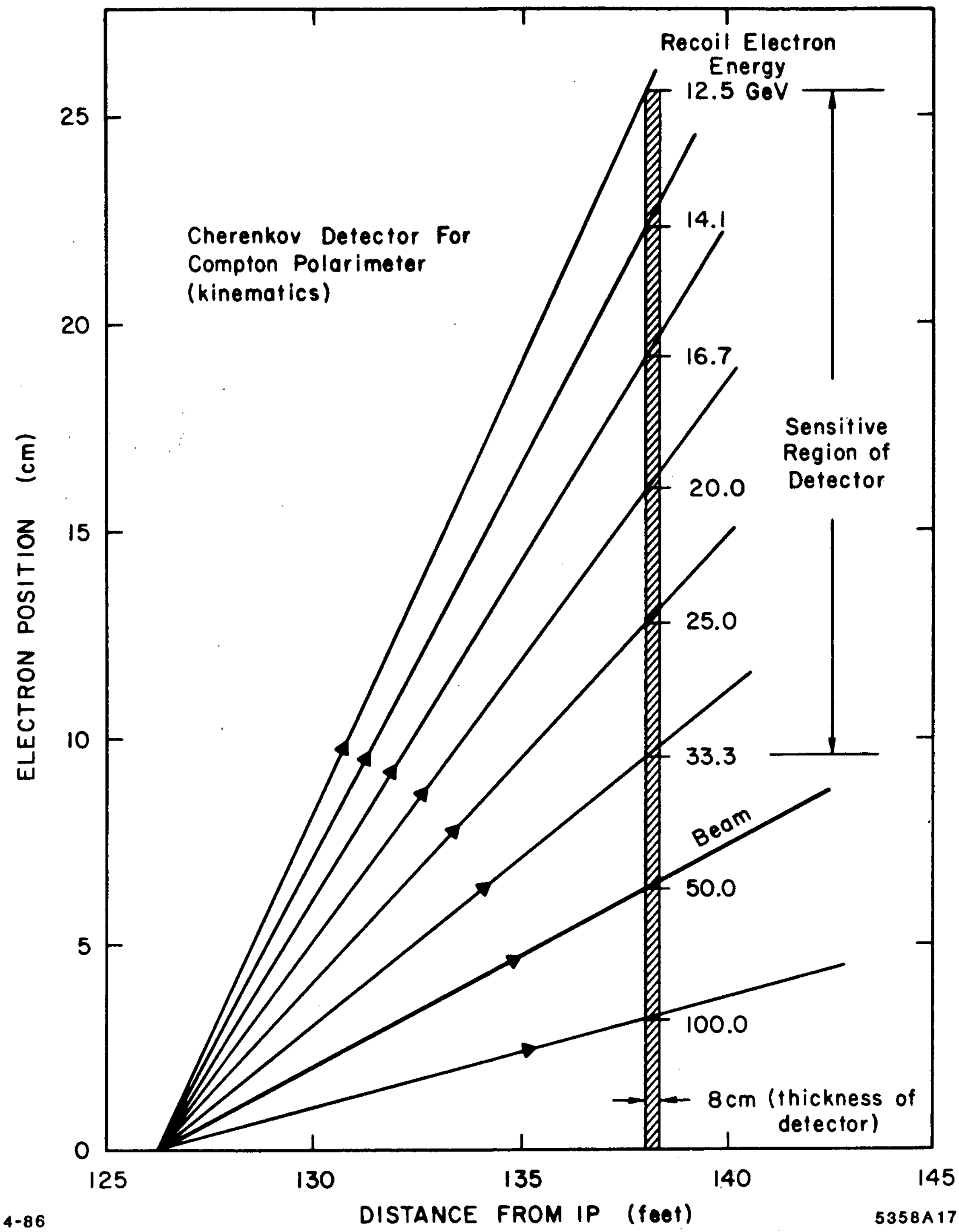
Recoil Electron
Energy
12.5 GeV
14.1
16.7
20.0
25.0
33.3
50.0
100.0
Beam
Cherenkov Detector For
Compton Polarimeter
(kinematics)
Sensitive
Region of
Detector
8cm (thickness of
detector)
ELECTRON POSITION (cm)
0
5
10
15
20
25
125
130
135
140
145
DISTANCE FROM IP (feet)
4-86
5358A17

Fig. 6

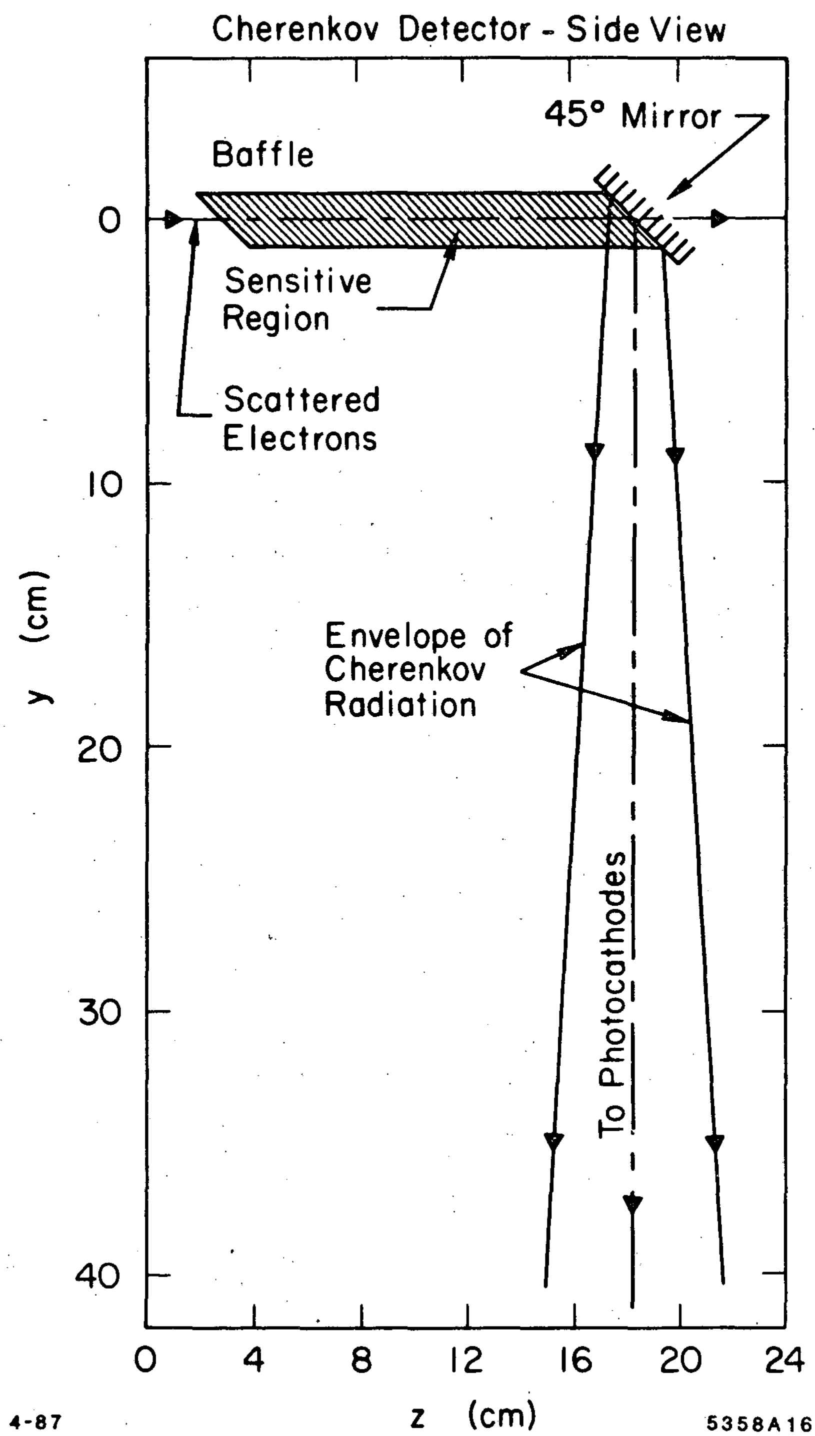

Cherenkov Detector - Side View
45° Mirror
Baffle
Sensitive
Region
Scattered
Electrons
Envelope of
Cherenkov
Radiation
To Photocathodes
y (cm)
0
10
20
30
40
0
4
8
12
16
20
24
z (cm)
4-87
5358A16

Fig. 7

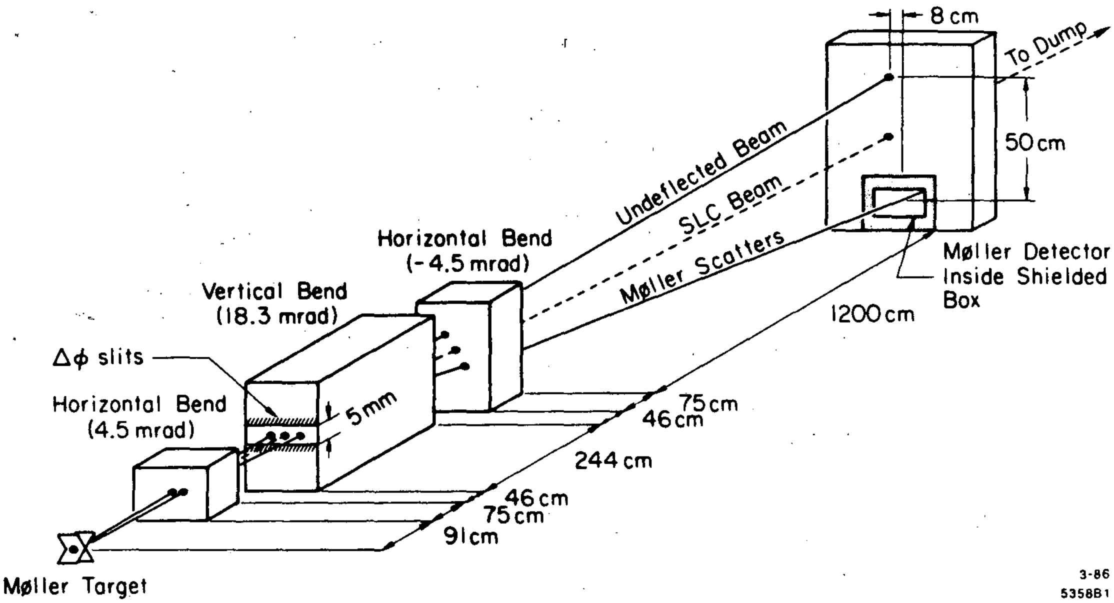

8 cm
To Dump
50 cm
Undeflected Beam
SLC Beam
Møller Scatters
Horizontal Bend
(-4.5 mrad)
Vertical Bend
(18.3 mrad)
Δφ slits
Horizontal Bend
(4.5 mrad)
5 mm
Møller Detector
Inside Shielded
Box
1200 cm
75 cm
46 cm
244 cm
46 cm
75 cm
91 cm
Møller Target
3-86
5358B1

Fig. 8

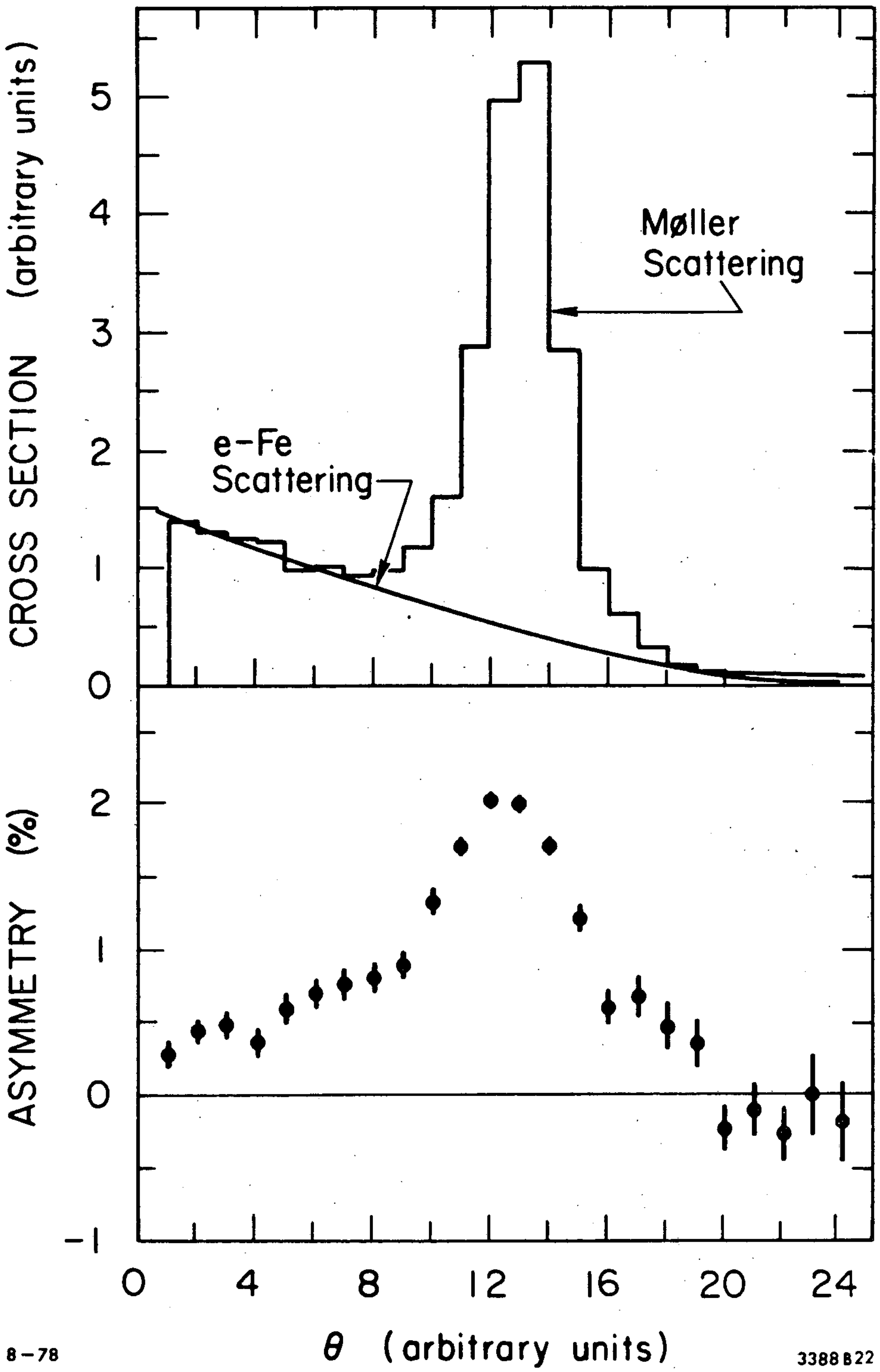
CROSS SECTION (arbitrary units)
5
4
3
2
1
0
Møller Scattering
e-Fe Scattering
ASYMMETRY (%)
2
1
0
-1
0
4
8
12
16
20
24
8-78
θ (arbitrary units)
3388B22

Fig. 9

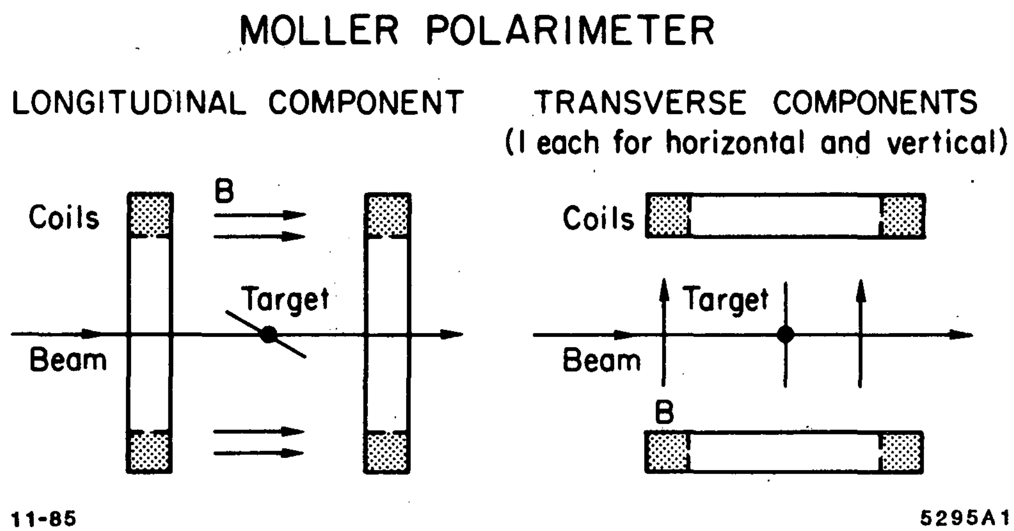
MOLLER POLARIMETER
LONGITUDINAL COMPONENT
TRANSVERSE COMPONENTS
(I each for horizontal and vertical)
Coils
B
Target
Beam
Coils
Target
Beam
B
11-85
5295A1

Fig. 10

MOLLER DETECTOR

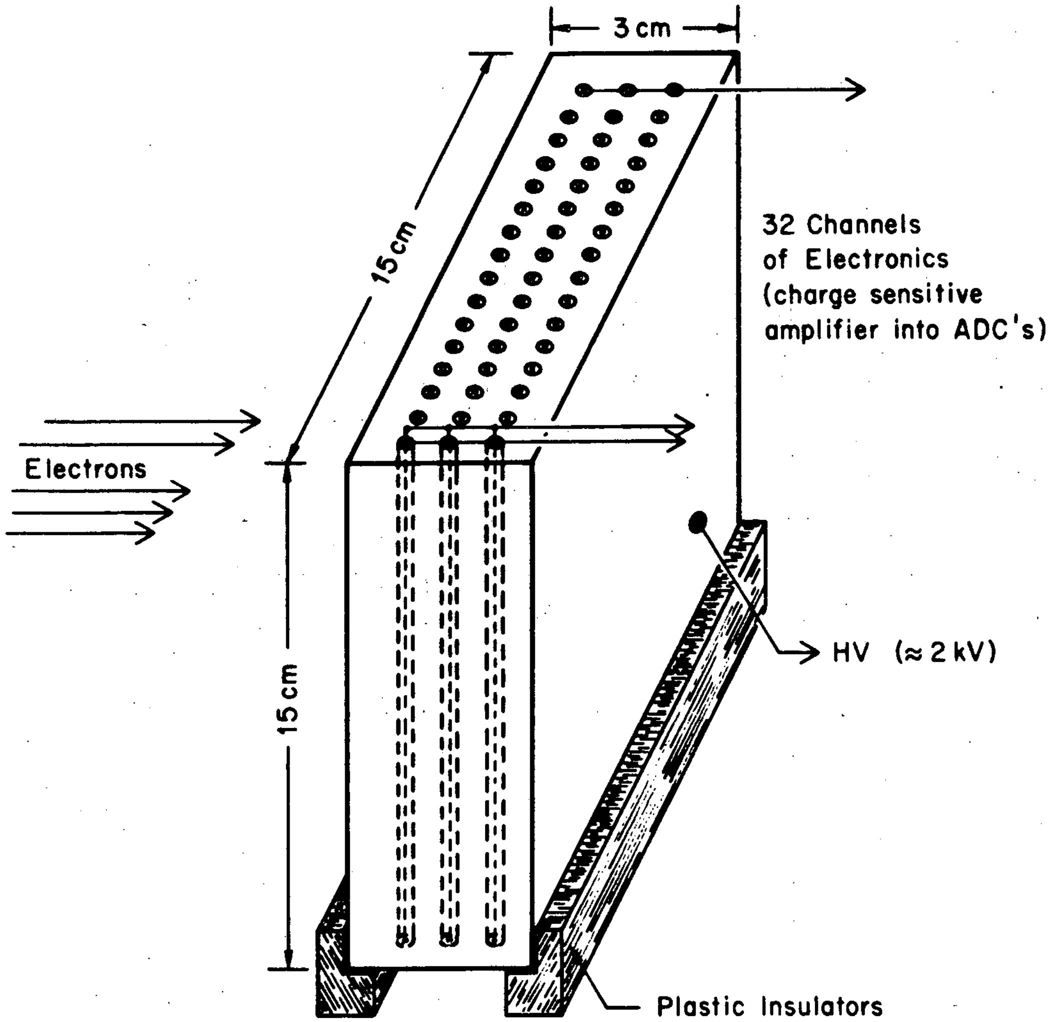

Gas: Argon Ethane
Material: Copper, Brass or Pb
Sense Wire: 20 micron W
Holes: 2mm Dia. Center-to-Center, 3mm Laterally, 1cm Longitudinally

12-85 5295A3

Fig. 11